IEEE Access
Multidisciplinary ⋮ Rapid Review ⋮ Open Access Journal

Received January 6, 2021, accepted January 17, 2021, date of publication January 19, 2021, date of current version January 27, 2021.

Digital Object Identifier 10.1109/ACCESS.2021.3052883

Guidance Simulation and Experimental Verification of Trajectory Correction Mortar Projectile

XITONG SUN[1], MIN GAO[1], XIAODONG ZHOU[1], JING LV[1], FENG TIAN[2], AND ZHIMING QIAO[1]
[1]Army Engineering University, Shijiazhuang Campus, Shijiazhuang 050003, China
[2]Beijing Institute of Aerospace Automatic Control, Beijing 100854, China

Corresponding author: Xiaodong Zhou (zhouxiaodong202010@163.com)

This work was supported by the Military Scientific Research Supports under Project ZS2015070132A12012.

ABSTRACT Integrated methods are used in the modification of trajectory, including improved perturbation impact point deviation prediction, adaptive proportional guidance and adaptive proportional differential guidance, thus improving the firing accuracy of guided mortar shell. The six degrees of freedom of both the trajectory model and the control model were established, and their guidance laws were designed based on the three guidance schemes. Firstly, the perturbation impact point deviation prediction method is improved by setting up a discrimination factor in the rising phase of trajectory based on the principle of traditional perturbation impact point deviation prediction method and in combination with the trajectory characteristics of guided mortar, which further improves the correction efficiency. The adaptive proportional guidance law is designed in the longitudinal plane, while the adaptive proportional differential guidance law is designed in the transverse plane due to the fact that the constant proportional coefficient in the proportional guidance law does not conform to the requirements of actual trajectory. In this paper, Monte Carlo simulation method and ammunition flight test are used to verify the designed guidance law, and the simulation results illustrate that the integrated guidance method is both reasonable and effective. As for the error of the guidance tool and actuator, the method is available for the reduction of impact point deviation and the improvement of accuracy. The circular error probability (CEP) not under control decreases from 126.317m to 10.1284m when control is applied. Besides, the feasibility of the designed guidance law is verified by the flight tests of guided mortar projectile in large, medium and small range respectively from the perspective of engineering application. It can be seen from the test trajectory impact point data that the guidance law is available for the effective correction of trajectory deviation in the actual hardware operation and site environment with reliable guidance. As the outcome, the CEP reaches 10.86m, and the impact point deviation of some guided missiles is within 2m.

INDEX TERMS Guidance, impact point deviation, proportional guidance, perturbation guidance, proportional differential.

I. INTRODUCTION

Functioning not only as an extremely important conventional weapon for army infantry but also a suppressive weapon to accompany and support infantry combat, mortar shell is capable of striking all kinds of active forces, armored targets and artillery positions at the front in shallow and certain depth. Unfortunately, most of the mortar shells in active service are uncontrollable, and suffer from various random interferences with their falling points scattered widely, which make it difficult for them to meet the demands of modern war [1], [2]. Therefore, guided transformation of mortar shells has become an important direction of development. On the other hand, the guidance elements are limited and miniaturized due to the limited space volume, and most control actuators are of pneumatic type with small volume. Besides, the detection element is composed of satellite receiver, ins and seeker [3]–[5]. With the guidance transformation of mortar

The associate editor coordinating the review of this manuscript and approving it for publication was Dipankar Deb.

shell hardware, various guidance methods are developed continuously.

In the references of [6]–[10], the offset term was designed to restrict the attack angle and fulfill the requirements of attacking the top with large angle of fall according to the traditional proportional navigation as well as the target characteristics and operational requirements. The content of References [11]–[13] includes the study of the application of the perturbed impact point prediction guidance method in guided ammunition, the analysis of the basic principle of the perturbed impact point prediction, the design of the relevant simulation experiments, and the verification of the effectiveness of the algorithm. In References [14]–[17], the trajectory correction projectile was taken as the research object, and the impact point prediction guidance algorithm and Kalman filter were applied for further improvement of the prediction accuracy. As per the simulation, the landing point prediction algorithm is available for the effective improvement of the impact point accuracy, besides, References [18]–[26] were based on the traditional proportional navigation algorithm. Offset term improvement and intercept angle model design were adopted to improve the guidance algorithm, and the effectiveness of the designed algorithm was verified by simulation according to the requirements of guidance ammunition's combat technical index, including the conditions of impact angle constraint, field of view angle constraint, overload constraint and initial leading angle, as well as the methods of over gravity compensation. In References [27]–[29], the study, design and verification of the guidance algorithm was implemented using optimal guidance law, sliding mode control or other methods, and based on the requirements of the constraint in terms of impact angle and attitude. In References [30]–[32], the nonlinear proportional navigation law is improved. Target related parameters is considered as unknown and hence estimated using disturbance observer. Sliding mode control is used for design of the control law. The stability of the proposed controller is then established using Lyapunov function. The effectiveness of the new control law is proved through simulations under various target maneuvering conditions. Nevertheless, this kind of algorithm was not suitable for the engineering application in low-cost missile propellant due to its higher complicity, hardware requirements, and demands for parameters in quantity.

Though both perturbation guidance and proportional guidance are available for the effective improvement of the firing accuracy of guided mortar projectiles, the current researches of perturbation guidance mainly focus on the convergence speed and accuracy of prediction deviation as well as the guidance effect when perturbation impact point deviation guidance law is applied alone. In the research of proportional navigation, as mentioned above, the proportional guidance law is designed based on the theory of constraint conditions or optimal control in most cases, which is mainly theoretical research, and difficult to be applied in engineering. The method which integrates improved perturbation impact point deviation prediction, adaptive proportional guidance and adaptive proportional differential guidance was designed in this paper to realize the engineering application of trajectory correction of guided mortar projectile. Besides, the discrimination factor was set up in the rising phase of trajectory according to the traditional perturbation guidance and the trajectory characteristics of guided mortar projectile. Adjustment achieved by means of positive or negative discriminant factor was applied to the rudder control phase. Longitudinal plane adaptive proportional navigation and transverse plane adaptive proportional differential guidance were designed based on proportional navigation. Using Monte Carlo simulation for shooting and flight test, the rationality and effectiveness of the integrated guidance law were verified when the error of guidance tools and actuators as well as the actual field environment were taken into account.

II. MODELING OF PROJECTILE MOTION MODEL

A. DYNAMIC EQUATION OF PTOJECTILE CENTROID MOTION

The dynamic equation of projectile centroid motion is established in ballistic coordinate system, as shown below [33], [34]:

$$\begin{cases} m\dfrac{dV}{dt} = G_{x_2} + R_{x_2} \\ mV\dfrac{d\theta}{dt} = G_{y_2} + R_{y_2} \\ -mV\cos\theta\dfrac{d\psi_v}{dt} = G_{z_2} + R_{z_2} \end{cases} \tag{1}$$

where, m——refers to projectile mass;

V—-refers to projectile velocity;

t—-refers to time;

θ—-refers to trajectory inclination angle;

ψ_v—-refers to ballistic deflection angle;

$G_{x_2}, G_{y_2}, G_{z_2}$—-refer to the component of gravity in ballistic coordinate system respectively;

$R_{x_2}, R_{y_2}, R_{z_2}$—-refer to the component of aerodynamic force in ballistic coordinate system respectively.

B. DYNAMIC EQUATION OF PTOJECTILE ROTATING AROUND THE CENTER OF MASS

The kinetic equation of projectile rotating around the center of mass is established in the quasi projectile coordinate system, as shown below [33], [34]:

$$\begin{bmatrix} J_{x_4}\dfrac{d\omega_{x_4}}{dt} \\ J_{y_4}\dfrac{d\omega_{y_4}}{dt} \\ J_{z_4}\dfrac{d\omega_{z_4}}{dt} \end{bmatrix} = \begin{bmatrix} M_{x_4} \\ M_{y_4} \\ M_{z_4} \end{bmatrix} - \begin{bmatrix} 0 \\ \left(J_{x_4} - J_{z_4}\right)\omega_{x_4}\omega_{z_4} \\ \left(J_{y_4} - J_{x_4}\right)\omega_{x_4}\omega_{y_4} \end{bmatrix} \tag{2}$$

where, $J_{x_4}, J_{y_4}, J_{z_4}$——refer to the moment of inertia of the projectile to each axis of the quasi projectile coordinate system respectively;

$\omega_{x_4}, \omega_{y_4}, \omega_{z_4}$——refer to the component of rotational angular velocity ω on each axis of quasi projectile coordinate system respectively;

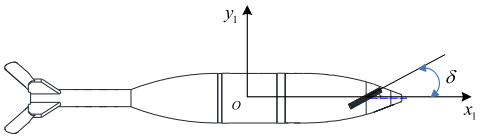

FIGURE 1. Schematic diagram of canards deflection.

$M_{x_4}, M_{y_4}, M_{z_4}$——refer to the component of aerodynamic moment in the quasi projectile coordinate system respectively.

C. KINEMATIC EQUATION OF PROJECTILE CENTROID MOTION

$$\begin{cases} \dfrac{dx}{dt} = V\cos\theta\cos\psi_V \\ \dfrac{dy}{dt} = V\sin\theta \\ \dfrac{dz}{dt} = -V\cos\theta\sin\psi_V \end{cases} \tag{3}$$

where x, y, z——refer to three axis coordinates of projectile in inertial system respectively [33], [34].

D. KINEMATICAL EQUATION OF PROJECTILE ROTATING AROUND THE CENTER OF MASS

$$\begin{cases} \dfrac{d\vartheta}{dt} = \omega_{z_4} \\ \dfrac{d\psi}{dt} = \dfrac{1}{\cos\vartheta}\omega_{y_4} \\ \dfrac{d\gamma}{dt} = \omega_{x_4} - \omega_{y_4}\tan\vartheta \end{cases} \tag{4}$$

where, ϑ——refers to pitch angle;
ψ——refers to yaw angle;
γ——refers to roll angle [33]–[35].

E. GEOMETRIC RELATION EQUATION

$$\begin{cases} \beta = \arcsin\left[\cos\theta\sin\left(\psi - \psi_v\right)\right] \\ \alpha = \vartheta - \arcsin\left(\dfrac{\sin\theta}{\cos\beta}\right) \\ \gamma_v = \arcsin\left(\tan\theta\tan\beta\right) \end{cases} \tag{5}$$

where, α——refers to angle of attack;
β——refers to sideslip angle;
γ_v——refers to velocity tilt angle [33], [34].

F. GOVERNIN EQUATION

Basic principles

A pair of rudder blades of the single-channel steering gear of the trajectory correction mortar is installed on the head of the projectile in zigzag, as shown in Fig. 1. The polarity of rudder deflection is positive when the leading edge of rudder piece is upward. On the other hand, the rudder deflection angle refers to the angle between the rudder piece and Ox_1 axis of missile body coordinate system.

The conventional control method for single-channel proportional electric actuator is divided into the following steps:

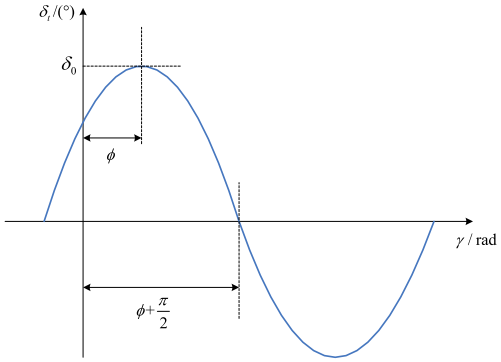

FIGURE 2. Canards deflection control signal.

firstly, convert the rudder offset track into the sinusoidal signal at the same frequency with the rotational speed; then, alter the magnitude and direction of the average control force by changing the amplitude and phase of the sinusoidal signal, and in this way to realize the control of pitch and yaw motion. The schematic diagram of control signal of the steering gear and rudder deviation is shown in Fig. 2 where δ_t refers to the real-time rudder control angle, δ_0 refers to the rudder control amplitude, γ refers to the missile roll angle, and ϕ refers to the rudder control phase. Besides, the variables in the figure satisfy the requirements of the relationship illustrated in Equation (6) [36], [37].

$$\delta_t = \delta_0 \cdot \sin(\gamma + \frac{\pi}{2} - \phi) \tag{6}$$

Because the missile body is characterized by low-pass filtering, the periodic average value of the control force generated by the deflection of the rudder plate is available to obtain the response from the missile body. Under the assumption that the actuator system works well without any time delay, and according to Formula (6), when the missile body rotates for one cycle, the equivalent pitch rudder angle and the equivalent yaw rudder angle are expressed as follows [37]:

$$\begin{aligned} \delta_z' &= \frac{1}{2\pi}\int_0^{2\pi} \delta_0 \cdot \sin(\gamma + \frac{\pi}{2} - \phi) \cdot \cos\gamma d\gamma \\ &= \frac{1}{2}\delta_0\cos\phi \end{aligned} \tag{7}$$

$$\begin{aligned} \delta_y' &= \frac{1}{2\pi}\int_0^{2\pi} \delta_0 \cdot \sin(\gamma + \frac{\pi}{2} - \phi) \cdot \sin\gamma d\gamma \\ &= \frac{1}{2}\delta_0\sin\phi \end{aligned} \tag{8}$$

The alteration of the amplitude and phase of rudder control will result in the changes of the equivalent pitch rudder angle and the equivalent yaw rudder angle. In other words, the alteration is available for the change of the magnitude and direction of the average control force generated by the steering gear.

The deflection of rudder has to be under control to eliminate the ballistic parameter deviation of longitudinal plane and transverse plane, and further to realize the two-dimensional correction of trajectory correction mortar shell.

Besides, set the deviation of ballistic parameters in longitudinal plane and transverse plane as ε_1 and ε_2 respectively, the pitch rudder control signal δ_z and yaw rudder control signal δ_y are generated in longitudinal plane and transverse plane. In that case, the value of δ_z depends on ε_1, and the value of δ_y depends on ε_2, that is,

$$\begin{cases} \delta_z = f(\varepsilon_1) \\ \delta_y = f(\varepsilon_2) \end{cases} \tag{9}$$

The rudder control amplitude and rudder control phase are calculated based on the pitch rudder control signal δ_z and the yaw rudder control signal δ_y. Therefore, the calculation method of rudder control amplitude was expressed as follows:

$$\delta_0 = \sqrt{\delta_y^2 + \delta_z^2} \tag{10}$$

Limited by the mechanical structure, with the maximum deflection amplitude of rudder set as $\delta'_{\max}$, it is necessary to limit the amplitude of δ_0, as shown below:

$$\begin{cases} \delta_0 = \delta'_{\max} & if(\delta_0 > \delta'_{\max}) \\ \delta_0 = \delta_0 & if(\delta_0 \le \delta'_{\max}) \end{cases} \tag{11}$$

Calculation of rudder control phase by Formula (12) and Equation (13) is expressed as follows [36], [37]:

$$\phi' = \begin{cases} \arctan\left(\dfrac{|\delta_y|}{|\delta_z|}\right) & |\delta_z| \ge |\delta_y| \\ \dfrac{\pi}{2} - \arctan\left(\dfrac{|\delta_z|}{|\delta_y|}\right) & |\delta_z| < |\delta_y| \end{cases} \tag{12}$$

where ϕ' refers to the intermediate variable for calculating rudder control phase [37].

$$\phi = \begin{cases} \phi' & \delta_z \ge 0, \delta_y \ge 0 \\ \pi - \phi' & \delta_z < 0, \delta_y \ge 0 \\ \pi + \phi' & \delta_z < 0, \delta_y < 0 \\ 2\pi - \phi' & \delta_z \ge 0, \delta_y < 0 \end{cases} \tag{13}$$

III. IMPROVED PREDICTIVE GUIDANCE METHOD FOR PERTURBED IMPACT POINT DEVIATION

A. PREDICTION PRINCIPLE OF PERTURBED IMPACT POINT PREDICTION ALGORITHM

According to the theory of external ballistics, the coordinates of impact point can be considered as the functions of ballistic coordinates and velocities at any time on the trajectory of projectiles, and so is the reference trajectory. Besides, the functional relationship between the coordinates of the impact point of the reference trajectory and the position (x_c, y_c, z_c) as well as the velocity (v_{xc}, v_{yc}, v_{zc}) of the reference ballistic projectile can be expressed as:

$$\begin{cases} X_C = L(v_{xc}, v_{yc}, v_{zc}, x_c, y_c, z_c) \\ Z_C = H(v_{xc}, v_{yc}, v_{zc}, x_c, y_c, z_c) \end{cases} \tag{14}$$

where, L refers to the range function, and H refers to the transversal function.

Similarly, the relationship among the coordinates of the impact point of the actual trajectory and the actual projectile position (x, y, z) as well as the actual projectile velocity (v_x, v_y, v_z) can be expressed as follows:

$$\begin{cases} X = L(v_x, v_y, v_z, x, y, z) \\ Z = H(v_x, v_y, v_z, x, y, z) \end{cases} \tag{15}$$

The existence of ballistic state deviation will cause the actual ballistic impact point to deviate from the reference ballistic impact point.

The deviation of impact point between actual trajectory and the reference one can be expressed as range deviation ΔL and lateral deviation ΔH, as expressed by the following equations:

$$\begin{cases} \Delta L = X - X_C \\ \Delta H = Z - Z_C \end{cases} \tag{16}$$

As per the perturbation theory, the actual trajectory makes a ''swing'' near the reference trajectory in small amplitude. In that case, the function of range and lateral deflection can be expanded by means of Taylor expansion on the reference trajectory, and the predicted impact point deviations of ΔL and ΔH can be obtained. The calculation formulas are expressed as follows:

$$\begin{cases} \Delta L = \dfrac{\partial L}{\partial \mathbf{v}^T}\Delta\mathbf{v} + \frac{\partial L}{\partial \mathbf{p}^T}\Delta\mathbf{p} + \Delta L^{(R)} \\ \Delta H = \dfrac{\partial H}{\partial \mathbf{v}^T}\Delta\mathbf{v} + \dfrac{\partial H}{\partial \mathbf{p}^T}\Delta\mathbf{p} + \Delta H^{(R)} \end{cases} \tag{17}$$

where

$$\frac{\partial L}{\partial \mathbf{v}^T} = \left(\frac{\partial L}{\partial v_x}\frac{\partial L}{\partial v_y}\frac{\partial L}{\partial v_z}\right) \tag{18}$$

$$\frac{\partial L}{\partial \mathbf{p}^T} = \left(\frac{\partial L}{\partial x}\frac{\partial L}{\partial y}\frac{\partial L}{\partial z}\right) \tag{19}$$

$$\frac{\partial H}{\partial \mathbf{v}^T} = \left(\frac{\partial H}{\partial v_x}\frac{\partial H}{\partial v_y}\frac{\partial H}{\partial v_z}\right) \tag{20}$$

$$\frac{\partial H}{\partial \mathbf{p}^T} = \left(\frac{\partial H}{\partial x}\frac{\partial H}{\partial y}\frac{\partial H}{\partial z}\right) \tag{21}$$

$$\Delta\mathbf{v} = \begin{bmatrix} v_x - v_{xc} \\ v_y - v_{yc} \\ v_z - v_{zc} \end{bmatrix} \tag{22}$$

$$\Delta\mathbf{p} = \begin{bmatrix} x - x_c \\ y - y_c \\ z - z_c \end{bmatrix} \tag{23}$$

In Equation (17), $\Delta L^{(R)}$ and $\Delta H^{(R)}$ refer to the higher-order terms of Taylor expansion.

Provided that the main factors affecting the range deviation and lateral deviation are taken into consideration only, the calculation formulas of range deviation and lateral deviation

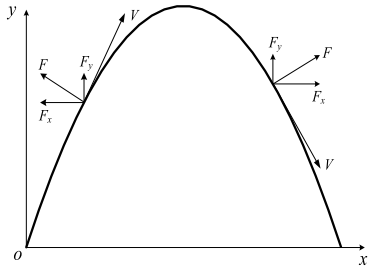

FIGURE 3. The force analysis of longitudinal trajectory correction.

will be given as follows:

$$\begin{cases} \Delta L = \dfrac{\partial L}{\partial v_x}\Delta v_x + \dfrac{\partial L}{\partial v_y}\Delta v_y + \dfrac{\partial L}{\partial y}\Delta y \\ + \dfrac{\partial^2 L}{\partial vx\partial v_y}\Delta v_x\Delta v_y + \dfrac{\partial^2 L}{\partial vx\partial y}\Delta v_x\Delta y + \dfrac{\partial^2 L}{\partial vy\partial y}\Delta v_y\Delta y \\ + \left(\dfrac{\partial^2 L}{\partial vx^2}\Delta v_x^2 + \dfrac{\partial^2 L}{\partial vy^2}\Delta v_y^2 + \dfrac{\partial^2 L}{\partial y^2}\Delta y^2\right)/2 \\ \Delta H = \dfrac{\partial H}{\partial v_z}\Delta V_z + \dfrac{\partial H}{\partial z}\Delta z \end{cases} \tag{24}$$

where $\partial L/\partial v_x$, $\partial L/\partial v_y$, $\partial L/\partial y$, $\partial L^2/\partial v_x\partial v_y$, $\partial L^2/\partial v_x\partial y$, $\partial L^2/\partial v_y\partial y$, $\partial L^2/\partial v_x^2$, $\partial L^2/\partial v_y^2$ and $\partial L^2/\partial y^2$ refer to the partial derivatives and second-order partial derivatives of range with respect to the ballistic height, longitudinal velocity and vertical component velocity.

B. CONVENTIONAL PREDICTIVE GUIDANCE METHOD FOR PERTURBED IMPACT POINT DEVIATION

With ΔL and ΔH taken as the control variable by the longitudinal and the transverse plane guidance loop respectively in the predictive guidance method of perturbed impact point deviation, the calculation method of pitch rudder control angle and yaw rudder control angle can be expressed as follows [13], [38], [39]:

$$\begin{cases} \delta_z = -k_L \cdot K_1 \cdot \Delta L \\ \delta_y = -k_H \cdot K_1 \cdot \Delta H \end{cases} \tag{25}$$

where k_L refers to the longitudinal amplification factor, k_H refers to the lateral amplification factor, and K_1 refers to the guidance system gain.

C. IMPROVEMENT OF PREDICTIVE GUIDANCE METHOD FOR PERTURBED IMPACT POINT DEVIATION

The actuator control force F can be decomposed into F_x and F_y in the launching coordinate system when the equivalent pitch rudder angle δ_z' is positive, and $Oxyz$ refers to the transmitting coordinate system, as shown in Fig. 3. When F_x is negative in the rising arc phase of trajectory, both the horizontal velocity of projectile and the range will be reduced. While, in the case that F_y is positive, the stagnation time of projectile and the range will be increased. The two functions are opposite, and the range-reduction effect of F_x is greater than that of F_y. Therefore, it is possible that the start and control time is early and the correction ability is reduced[40].

It can be concluded from the above analysis that no single corresponding relationship exists between the equivalent pitch rudder angle and the range correction effect. Besides, a positive equivalent pitch rudder angle may not increase the range, and the correction effect of equivalent pitch rudder angle on range is related to the motion state of projectile [36].

Assume that the control is started from time t and time Δt is applied, then set the equivalent pitch rudder angle as δ_z'. The deflection of rudder plate will result in the changes of the drag, lift and lateral force of missile body, and ΔX, ΔY, ΔZ are used to represent the modified variables respectively.

In that case, the control force produced by rudder deflection can be expressed as follows:

$$\begin{bmatrix} F_{x2} \\ F_{y2} \\ F_{z2} \end{bmatrix} = \begin{bmatrix} -\Delta X \\ \Delta Y\cos\gamma_V - \Delta Z\sin\gamma_V \\ \Delta Y\sin\gamma_V + \Delta Z\cos\gamma_V \end{bmatrix} \tag{26}$$

where F_{x2}, $F_{y2}F_{z2}$ refer to the axial component of the control force generated by the steering gear in the ballistic coordinate system respectively.

For longitudinal correction, $\Delta Z \approx 0$. In addition, the increment of air resistance is smaller than that of normal force without any obvious effect on the range. It can also be considered as 0, that is, $\Delta X \approx 0$. Besides, γ_V is taken a small amount, and $\cos\gamma_V \approx 1$, $\sin\gamma_V \approx 0$. Therefore, Equation (23) can be rewritten as follows:

$$\begin{bmatrix} F_{x2} \\ F_{y2} \\ F_{z2} \end{bmatrix} = \begin{bmatrix} 0 \\ \Delta Y \\ 0 \end{bmatrix} = \begin{bmatrix} 0 \\ c_y^{\delta_z'}\delta_z qSL \\ 0 \end{bmatrix} \tag{27}$$

where $c_y^{\delta_z'}$ refers to the partial derivative of lift coefficient to the equivalent pitch rudder angle.

The projection of the actuator control force in the launching system can be expressed as follows:

$$\begin{bmatrix} F_x \\ F_y \\ F_z \end{bmatrix} = C_2^f \begin{bmatrix} F_{x2} \\ F_{y2} \\ F_{z2} \end{bmatrix} = \begin{bmatrix} -F_{y2}\sin\theta\cos\psi_V \\ F_{y2}\cos\theta \\ \sin\theta\sin\psi_V \end{bmatrix} \tag{28}$$

where F_x, F_y, F_z refer to the axis component of the steering gear control force in the launching coordinate system respectively;

C_2^f refers to the matrix for the transformation from the ballistic coordinate system to the launch coordinate system.

Since ψ_V was small, $\cos\psi_V \approx 1$, $\sin\psi_V \approx 0$, Equation (25) can be rewritten as follows:

$$\begin{bmatrix} F_x \\ F_y \\ F_z \end{bmatrix} = \begin{bmatrix} -F_{y2}\sin\theta \\ F_{y2}\cos\theta \\ 0 \end{bmatrix} \tag{29}$$

Let Δt be short enough to keep F_{y2} constant for Δt time. Then, after time Δt, the projectile will obtain velocity and position increment.

The speed increment can be expressed as follows:

$$\begin{bmatrix} \Delta v_x \\ \Delta v_y \\ \Delta v_z \end{bmatrix} = \begin{bmatrix} -F_{y2}\sin\theta\Delta t/m \\ F_{y2}\cos\theta\Delta t/m \\ 0 \end{bmatrix} \tag{30}$$

where $\Delta v_x, \Delta v_y, \Delta v_z$ refer to the axial component of the velocity increment of the projectile in the launching system when the actuator acts for Δt time.

The position increment can be expressed as follows:

$$\begin{bmatrix} \Delta x \\ \Delta y \\ \Delta z \end{bmatrix} = \begin{bmatrix} -F_{y2} \sin\theta (\Delta t)^2/(2m) \\ F_{y2} \cos\theta (\Delta t)^2/(2m) \\ 0 \end{bmatrix} \tag{31}$$

where $\Delta x, \Delta y, \Delta z$ refer to the axial component of the projectile's position increment in the launching system when the actuator acts for Δt time.

The velocity and position increment obtained by the projectile will eventually have their impact on the projectile range. On the other hand, according to the perturbation theory, the impacts of velocity and position increment on the range of projectile can be expressed as follows:

$$\delta L = \frac{\partial L}{\partial v_x}\Delta v_x + \frac{\partial L}{\partial v_y}\Delta v_y + \frac{\partial L}{\partial x}\Delta x + \frac{\partial L}{\partial y}\Delta y \tag{32}$$

where $\partial L/\partial x$ refers to the partial derivative of range to horizontal position, and δL refers to the range correction obtained by Δt time of actuator action.

By introducing Equation (30) and Equation (31) into Equation (32), it can be obtained as follows:

$$\begin{aligned} \delta L = {} & \frac{\partial L}{\partial v_x}\left(\frac{-F_{y2}\sin\theta}{m}\Delta t\right) + \frac{\partial L}{\partial v_y}\left(\frac{F_{y2}\cos\theta}{m}\Delta t\right) \\ & + \frac{\partial L}{\partial x}\left[\frac{-F_{y2}\sin\theta}{2m}(\Delta t)^2\right] + \frac{\partial L}{\partial y}\left[\frac{F_{y2}\cos\theta}{2m}(\Delta t)^2\right] \end{aligned} \tag{33}$$

In Equation (33), $(\Delta t)^2$ is a second-order small quantity, which can be ignored, in that case, Equation (33) can be rewritten as follows:

$$\delta L = \frac{F_{y2}\Delta t}{m}\left(\frac{\partial L}{\partial v_y}\cos\theta - \frac{\partial L}{\partial v_x}\sin\theta\right) \tag{34}$$

where, δL indicates the correction effect of the steering gear on the range; when δL is positive, it means that the range is increased, vice versa, when δL is negative, it means that the range is reduced.

By introducing Equation (27) into Equation (34), we can get:

$$\delta L = \frac{c_y^{\delta'_z}\delta'_z qSL\Delta t}{m}\left(\frac{\partial L}{\partial v_y}\cos\theta - \frac{\partial L}{\partial v_x}\sin\theta\right) \tag{35}$$

Equation (35) acts as the model for range correction by equivalent pitch rudder angle.

It can be seen from Equation (35) that the correction effect of the equivalent rudder angle on the range doesn't depend on the equivalent rudder angle itself, but also on the aerodynamic parameters, structural parameters and motion state of the missile body. On the other hand, from the perspective of flight control, the main concern lies in the positive and negative effects of equivalent pitch rudder angle on range correction. For this reason, the variable a is defined as the discriminant factor, as shown below.

$$a = \left(\frac{\partial L}{\partial v_y}\cos\theta - \frac{\partial L}{\partial v_x}\sin\theta\right) \tag{36}$$

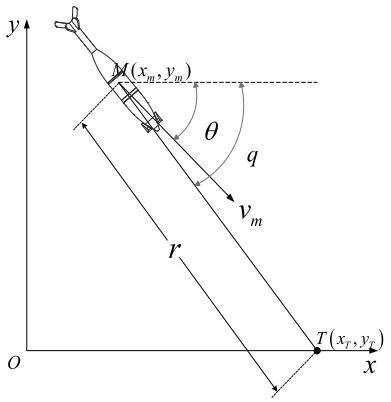

FIGURE 4. Schematic diagram of projectile-target relationship.

By introducing Equation (36) into (35), we can get

$$\delta L = \frac{c_y^{\delta'_z} qSL\Delta t}{m}\delta'_z a \tag{37}$$

In Equation (37), $c_y^{\delta'_z}, m, q, S, L, \Delta t$ are greater than 0, besides, whether δL is positive or negative mainly depends on the positive and negative characteristics of δ'_z and a, that is, when a is positive, the positive or negative of δL is the same as that of δ'_z. In contrast, in the cast that a is negative, the positive and negative of δL is opposite to that of δ'_z.

Before firing, $\partial L/\partial v_x, \partial L/\partial v_y$ are fixed to the missile borne computer which interpolates the corresponding value according to the position of the projectile. Besides, the trajectory angle θ is calculated by the velocity value measured by the satellite navigation and positioning receiver.

Based on discriminant factor and the model of range correction by equivalent pitch rudder angle, an improved perturbation impact point deviation prediction guidance method was proposed as follows.

$$\begin{cases} \delta_z = -k_L \cdot K_1 \cdot \Delta L & if(a > 0) \\ \delta_z = k_L \cdot K_1 \cdot \Delta L & if(a \le 0) \\ \delta_y = -k_H \cdot K_1 \cdot \Delta H \end{cases} \tag{38}$$

Compared with Equation (25), the improved predictive guidance method of perturbation impact point deviation has the advantage that the longitudinal trajectory correction is no longer limited to the trajectory descent phase. As long as the mortar projectile meets the requirements of stability conditions and the guidance system is ready, the longitudinal trajectory correction can be started. While in the ascent phase of trajectory, the rudder control phase is adjusted by the positive and negative value of the discrimination factor a, which is available to improve the correction ability of the ascent phase and realize the correction effect of the actuator on the range in the whole trajectory phase.

IV. PROPORTIONAL GUIDANCE LAW

A. GUIDANCE PRINCIPLE OF PROPORTIONAL GUIDANCE LAW

The relative motion relationship between the projectile and the target point in the longitudinal plane was shown in Fig. 4.

Suppose the target point is T, and the coordinate is (x_T, y_T). M represents the real-time position of the projectile, and the coordinates are represented by (x_m, y_m). q is line of sight angle, and θ is trajectory angle.

As defined by the proportional navigation law, the angular rate of projectile velocity rotation is in direct proportion to the angular rate of line of sight rotation. In the meantime, the following equation should be followed [33], [41]:

$$\begin{cases} \dot{\theta} = k_{PL}\dot{q}_L \\ \dot{\psi}_V = k_{PH}\dot{q}_H \end{cases} \tag{39}$$

where, $\dot{\theta}$ refers to the change rate of ballistic inclination angle, k_{PL} refers to the longitudinal plane proportional coefficient, $\dot{q}_L$ refers to the longitudinal plane line of sight angular rate; $\dot{\psi}_V$ refers to the ballistic deflection angle change rate, k_{PH} refers to the transverse plane proportional coefficient, and $\dot{q}_H$ refers to the transverse plane line of sight angular rate. On the other hand, $\dot{q}_L$ and $\dot{q}_H$ are calculated based on the position and velocity information of the projectile and the position information of the target point.

The calculation method is expressed as follows [36], [41]:

$$\begin{cases} \dot{q}_L = \dfrac{\Delta x \cdot v_{ym} - \Delta y \cdot v_{xm}}{D^2} \\ \dot{q}_H = \dfrac{\Delta x \cdot v_{zm} - \Delta z \cdot v_{xm}}{D^2} \end{cases} \tag{40}$$

where $(\Delta x, \Delta y, \Delta z)$ refers to the deviation between the projectile position and the target position. While D refers to the distance between the missile and the target. Besides, (v_{xm}, v_{ym}, v_{zm}) refers to the projectile velocity.

The calculation formula of the deviation $(\Delta x, \Delta y, \Delta z)$ between the projectile position and the target point is expressed as follows:

$$\begin{cases} \Delta x = x_T - x_m \\ \Delta y = y_T - y_m \\ \Delta z = z_T - z_m \end{cases} \tag{41}$$

The calculation formula of missile target distance D is obtained by the following equation:

$$D = \sqrt{\Delta x^2 + \Delta y^2 + \Delta z^2} \tag{42}$$

By integrating Equation (39), we can get

$$\begin{cases} \theta_{cx} = \theta_0 + k_{PL}(q_L - q_{L0}) \\ \psi_{V_{cx}} = \psi_{V_0} + k_{PH}(q_H - q_{H0}) \end{cases} \tag{43}$$

where θ_{cx} refers to the command trajectory inclination angle, $\psi_{V_{cx}}$ refers to the command trajectory deflection angle, θ_0 and ψ_{V_0} refer to the trajectory inclination angle and trajectory deflection angle at the beginning of proportional guidance respectively; besides, q_{L0} and q_{H0} refer to the longitudinal plane missile target line of sight angle and the transverse plane missile target line of sight angle at the beginning of proportional guidance respectively.

The formula for calculating the trajectory inclination angle and trajectory deflection angle based on the projectile position and velocity information is expressed as follows[36]

$$\begin{cases} \theta = tg^{-1}(\dfrac{v_{ym}}{v_{xm}}) \\ \psi_V = \sin^{-1}(\dfrac{-v_{zm}}{v_m}) \end{cases} \tag{44}$$

The longitudinal guidance signal is calculated based on the difference between the projectile trajectory inclination angle and the command trajectory inclination angle. While the lateral guidance signal is calculated based on the difference between the ballistic deflection angle of the projectile and that of the command trajectory [36]

$$\begin{cases} U_\theta = \theta - \theta_{cx} \\ U_{\psi_V} = \psi_V - \psi_{V_{cx}} \end{cases} \tag{45}$$

where U_θ refers to the longitudinal guidance signal, and U_{ψ_V} refers to the lateral guidance signal.

U_θ and U_{ψ_V} are taken as the control variables in the longitudinal plane guidance loop and the transverse plane guidance loop respectively. Besides, the calculation method of pitch rudder control angle and yaw rudder control angle is expressed as follows [36]:

$$\begin{cases} \delta_z = -k_L \cdot K_1 \cdot U_\theta \\ \delta_y = k_H \cdot K_1 \cdot U_{\psi_V} \end{cases} \tag{46}$$

$$K_1 = \frac{1}{K_M} \tag{47}$$

where K_M refers to the projectile transfer coefficient, k_L refers to the longitudinal amplification factor, and k_H refers to the transverse amplification factor.

B. LONGITUDINAL PLANE ADAPTIVE PROPORTIONAL NAVIGATION LAW

In this section, the reason why the command trajectory inclination angle formed by the guidance law does not conform to the change law of trajectory inclination angle is analyzed, and a longitudinal plane adaptive proportional guidance law is proposed [42].

It is assumed that the change rate of trajectory inclination angle is related to Los rate, as shown below:

$$\dot{\theta} = k'_{PL}\dot{q}_L \tag{48}$$

where k'_{PL} refers to the ratio between the trajectory angle change rate and the line of sight angle rate.

After that, the actual trajectory inclination angle can be expressed as follows:

$$\theta = \theta_0 + k'_{PL}(q_L - q_{L0}) \tag{49}$$

Substituting Equation (43) and Equation (49) into Equation (45), we can get

$$U_\theta = (k'_{PL} - k_{PL}) \cdot (q_L - q_{L0}) \tag{50}$$

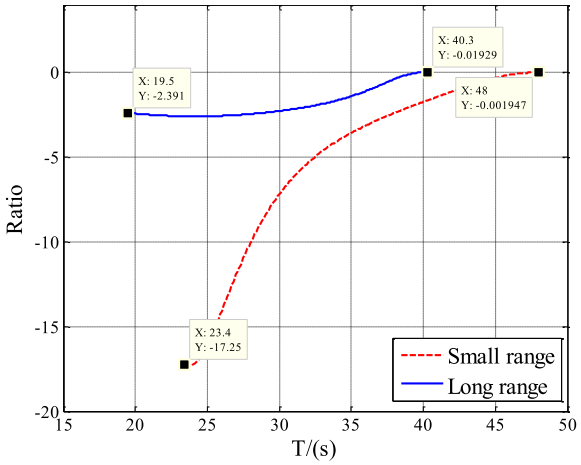

FIGURE 5. The ratio of trajectory incline angle change rate and line of sight angle change rate.

The pitch rudder control angle of the projectile can be expressed as follows[40]:

$$\delta_z = -k_L \cdot K_1 \cdot (k'_{PL} - k_{PL}) \cdot (q_L - q_{L0}) \tag{51}$$

In Equation (51), k_L and K_1 are selected according to ballistic characteristics. Although the change value, i.e., $(q_L - q_{L0})$ of missile target line of sight angle is subject to the control, the exterior trajectory of trajectory correction mortar shell is relatively stable, and the change obtained by $(q_L - q_{L0})$ of line of sight angle mainly depends on the relative motion characteristics of the projectile and the target. The required overload mainly depends on the difference between the proportional coefficient k_{PL} and k'_{PL} which refers to the ratio between the change rate of trajectory inclination angle and the rate of line of sight angle in actual trajectory due to the fact that the required overload corresponds to the control angle of pitch rudder [43].

The impact points of large-range trajectory (6.7 km range) and the small-range one (2.0 km range) are set as the target points respectively, and the ratio between the trajectory inclination angle change rate as well as the line of sight angle rate in the process of mortar projectile approaching target was calculated. As illustrated in Fig. 5, the ratio between the trajectory angle change rate and the line of sight angle rate changes smoothly at large range, which is -2.391 when entering the falling arc section, and about 0 when the projectile lands separately. In the case that the range is small, the ratio between the trajectory angle change rate and line of sight angle rate changes greatly, which is -17.25 when entering the falling arc section, and about 0 when the projectile lands respectively.

The trajectory bending characteristic of trajectory correction mortar shell is obvious, and it can be seen from Fig. 5 that the ratio between the trajectory angle change rate and the line of sight angle rate changes continuously based on the curved trajectory. The instruction ratio of guidance law has to be followed on a timely basis, and in the case that there is a big difference between the command ratio and the actual one, the correction ability will be reduced and the impact point deviation will be increased. Therefore, an adaptive proportional navigation law was proposed to solve this problem.

The method is schemed as follows: firstly, a standard trajectory centered on the target is determined by searching the firing angle. Besides, the ratio k'_{PL} between the trajectory angle change rate $\dot{\theta}'$ and the line of sight angle rate $\dot{q}'$ is calculated based on the trajectory information. It can be seen from Fig. 5 that k'_{PL} is not a fixed value but a variable based on the motion of the projectile. It is assumed that the proportional coefficient k_{PL} is always equal to k'_{PL} when the trajectory correction mortar projectile attacks the target. With the standard trajectory, the flight control system can hit the target without trajectory correction, therefore, if the scale factor k_{PL} is equal to k'_{PL}, the scale factor will match the ratio between the trajectory angle change rate and the line of sight angle rate of standard trajectory exactly.

Let the proportional coefficient k_{PL} be equal to k'_{PL} which is determined by the standard trajectory, as expressed in the following equation.

$$k_{PL} = k'_{PL} = \frac{\dot{\theta}'}{\dot{q}'_L} \tag{52}$$

C. GUIDANCE PRINCIPLE OF ADAPTIVE PROPORTIONAL DIFFERENTIAL GUIDANCE LAW

The main factor for the formation of the horizontal plane dispersion refers to the deviation of the shooting direction. While the formation characteristic of the lateral impact point deviation refers to the fact that the lateral impact point deviation increases gradually with the increase of flight time. Therefore, the rapid reduction of the lateral position deviation and the lateral velocity presents an effective way to reduce the lateral plane impact point deviation, and the adaptive proportional differential guidance law is adopted in the transverse plane. The calculation method of lateral guidance signal in proportional differential guidance law is described as follows

$$U_{\psi_V} = k_P \cdot z + k_P \cdot T_D \cdot v_z \tag{53}$$

where, k_P refers to the proportional coefficient, T_D refers to the differential time constant, z refers to the horizontal coordinates of projectile in inertial system and v_z refers to the lateral velocity of projectile in inertial system.

The purpose of the lateral control lies in the reduction of the deviation of lateral impact point which, caused by lateral velocity is related to the remaining flight time, therefore, the differential time constant is equal to the remaining flight time, and the adaptive variation of differential time constant is thus realized. That is

$$T_D = T_{go} \tag{54}$$

where, T_{go} refers to the remaining flight time.

The total flight time of reference trajectory is taken as the estimated total flight time of actual trajectory since the

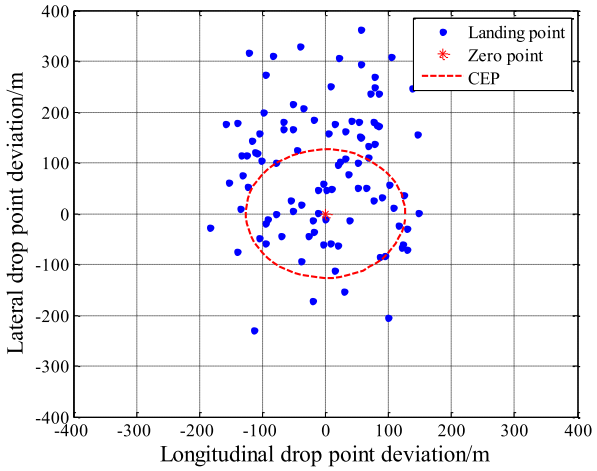

FIGURE 6. Shooting result of uncontrolled projectiles.

exterior trajectory of trajectory correction mortar shell is relatively stable and the flight time difference of different trajectory is small. The remaining flight time is obtained by subtracting the flight time from the total flight time of the reference trajectory.

$$T_{go} = T_z - t \tag{55}$$

where, T_z refers to the total flight time of the reference trajectory.

Since the actual flight time of the trajectory may be greater than the total flight time of the reference one, T_{go} is always made equal to 0 to make sure that T_{go} is always greater than or equal to 0 when the value of T_{go} is less than 0, as expressed in the following equation.

$$T_{go} = 0 \quad if \ (T_{go} < 0) \tag{56}$$

The calculation method of yaw rudder control angle is expressed as follows[36]:

$$\delta_y = -k_H \cdot K_1 \cdot U_{\psi_V} \tag{57}$$

V. SIMULATION ANALYSIS AND FLIGHT TEST

A. SETTING OF SIMULATION STATE IN SIMULATED SHOOTING

The target range was set at 6.7 km, while the initial velocity was set at 334 m/s, and the altitude was set at 265m to ensure that the simulated shooting range and ballistic characteristics were representative; besides, the standard meteorological conditions of artillery were adopted. The shooting angle was determined at 45 ° and the shooting direction was determined at 0.13 ° to the right according to the target range. Besides, the ballistic states of simulated shooting were obtained by the modification of the standard ballistic state of 6.7km range when various interferences were considered, with the interferences and their distribution law illustrated in Table. 1.

The simulated shooting was repeated for 100 times following the above simulation shooting process with the simulated shooting results shown in Fig. 6. The values of various interferences for each trajectory (100 in total) in the simulation

TABLE 1. The list of interference items.

Serial number	Interference term	Law of distribution	Numerical value (3σ)
1	Deviation of axial force coefficient/%	Normal distribution	±8.0
2	Deviation of normal force coefficient/%	Normal distribution	±5.0
3	Deviation of lateral force coefficient/%	Normal distribution	±5.0
4	Deviation of pitch moment coefficient/%	Normal distribution	±5.0
5	Deviation of yaw moment coefficient/%	Normal distribution	±5.0
6	Deviation of rolling moment coefficient/%	Normal distribution	±5.0
7	Angle deviation/°	Normal distribution	±0.8
8	Initial velocity deviation/(m/s)	Normal distribution	±5.0
9	Direction deviation/°	Normal distribution	±0.8
10	Wind speed/(m/s)	Normal distribution	5.0
11	Wind direction/°	Normal distribution	[0 360]

shooting were recorded and further used to simulate the interference of shooting. This method is available to make sure that the interference terms were kept the same regardless of shooting with or without control. The influence of different values of interference terms on the accuracy of impact point was thus eliminated.

The simulation results consist of the range of longitudinal impact point deviation of −314.4619m∼275.8603m, the range of lateral impact point deviation between −182.3914m∼148.7034m, the standard deviation of longitudinal impact point deviation of 126.5354m, the standard deviation of lateral deviation 84.9964m, and CEP of 126.317m.

B. SIMULATION OF TRAJECTORY CORRECTION EFFECT

The information of position and velocity for guided mortar projectile is obtained through satellite navigation, and that of the roll attitude is measured by geomagnetic attitude measurement component. The actuator is of a single channel proportional electric type, and various errors are involved in the simulation of simulated shooting of guided mortar projectile, including the position error, velocity error of satellite navigation and positioning receiver, geomagnetic angle measurement error and rudder deviation delay error, as illustrated in Table. 2.

Based on the analysis of the above guidance law, the improved perturbation impact point deviation prediction guidance was adopted in the longitudinal plane arc rising section, while the adaptive proportional guidance law was utilized in the longitudinal plane arc descending section; at last, the adaptive proportional differential guidance law was used in the transverse plane.

TABLE 2. Guide instrument and actuator errors.

Error term	Numerical value
Positioning error (1σ)	10 m
Speed error (1σ)	0.4 m/s
Roll angle measurement error (3σ)	5°
Rudder deflection delay (1σ)	1 ms

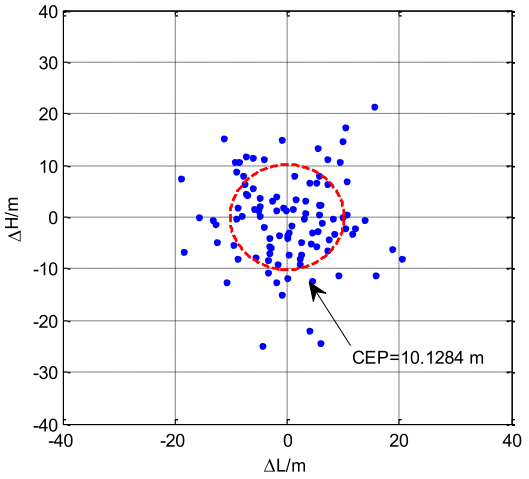

FIGURE 7. Impact point dispersion of controlled projectile.

With the start-up time set at 10s, when two kinds of guidance methods were used in the longitudinal plane, the condition of changing the guidance method from ascending to descending arc was $v_y < -10m/s$, so as to avoid the trajectory apex and the flight stability of the projectile, with the simulation results shown in Fig. 7.

The simulation results, i.e., the longitudinal standard deviation of 8.3572m, the transverse standard deviation of 8.8474m, and the CEP of 10.1284m, showed that the CEP obtained by flight control algorithm was available to meet the requirements of trajectory correction mortar shell combat technical index when various errors were taken into consideration.

C. FLIGHT TEST

The composite guidance flight test of guided mortar projectile was carried out to verify the guidance accuracy of the designed guidance method. In the experiment, ballistic radar and missile borne recorder were used to measure ballistic parameters, and five guided mortar rounds were launched. Besides, the coordinates of missile launching point and target point were illustrated in Table 3.

In the test, three shooting distances were selected, that is, large range of 6.7km, medium range of 5.5km and small range

TABLE 3. Coordinates of launching point and target point.

Place	WGS-84 coordinate system	
	longitude	latitude
Launch point	124°29′2.363″	47°30′8.289″
2.15km	124°30′42.34439″	47°30′52.10721″
	124°30′42.3317″	47°30′52.1893″
5.5km	124°33′20.41777″	47°30′25.605346″
6.7km	124°34′18.97534″	47°30′23.70302″
	124°34′18.3725″	47°30′23.7030″

TABLE 4. Units for magnetic properties.

Number	Target point	Landing point		Deviation	
	X(m)	X(m)	Z(m)	△L(m)	△H(m)
ZD1	6766.4	6755.7	10.3541	10.3541	-10.7203
ZD2	6754.1	6762.5	-0.3918	8.4535	-0.3918
ZD3	6754.1	6752	1.0738	-2.0591	1.0738
ZD4	5558.1	5543.6	-1.8921	-14.4641	-1.8921
ZD5	2149.9	2156	-7.5944	6.0857	-7.5944

of 2.15km. On the other hand, the altitude of the target and launch point were both 164m.

The impact point data of all guided mortar projectiles were illustrated in Table 4. Besides, the coordinates of the target point and the landing point were given within the launch coordinate system; and the z-direction coordinates of the target point were both 0m, which was not specially indicated in the table. The five missiles to be launched were numbered in the order of ZD1∼ZD5 respectively.

It can be seen from Table 4 that the impact point deviation of the 5-launch missiles is very small. Except for the fact that the deviation of ZD1 is slightly larger than 10m, and those of other missiles are less than 10m.The small-range ZD5 and the large-range ZD2 were selected to analyze the test data of 5-launch missiles. Besides, by covering the whole range, the large and small ranges are characterized by representativeness.

1) TEST DATA ANALYSIS OF LONG RANGE MISSILE

With the firing angle of 45° and the firing direction of 1695mil for ZD2, the actual range was 6762.5m and the range of target point was 6754.1m. Besides, the longitudinal

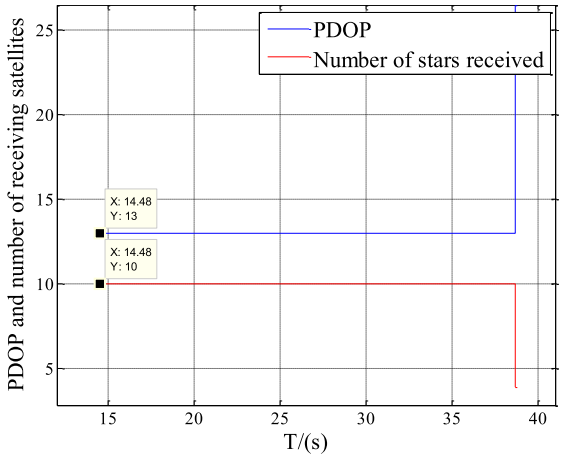

FIGURE 8. PDOP and the number of receiving satellites in large range.

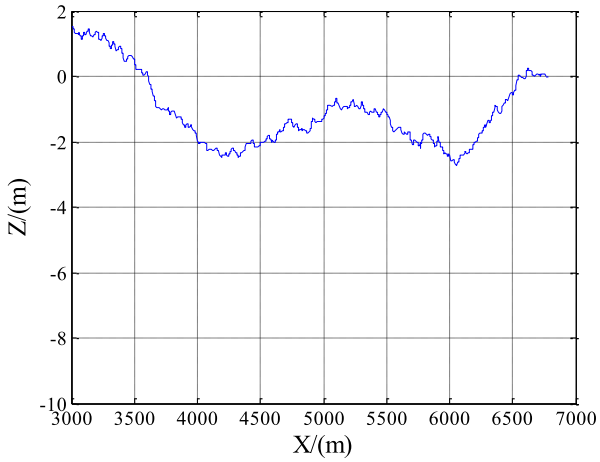

FIGURE 10. Range-Lateral deflection curve.

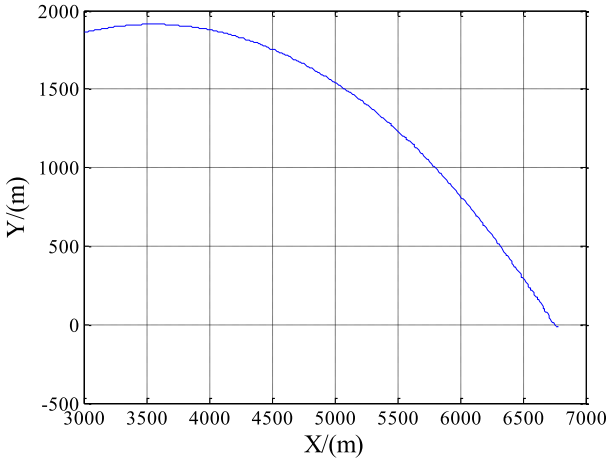

FIGURE 9. Range-Trajectory height curve.

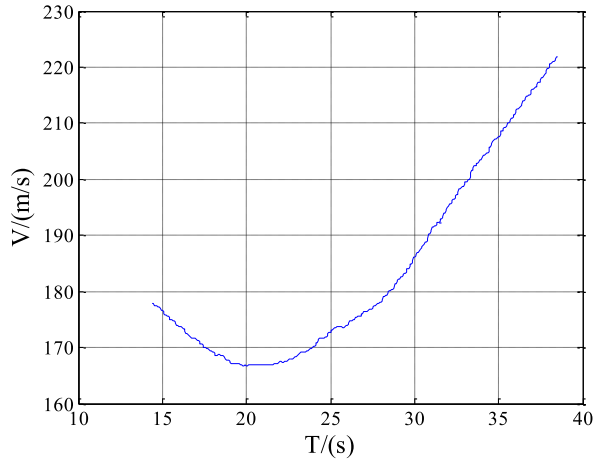

FIGURE 11. Time-Velocity curve.

deviation of the final impact point was 8.4535m, and the transverse deviation was −0.3918m. When being launched, the missile flew stably and landed normally, and the data of recorder was normal as well. PDOP and star number were shown in Fig. 8.

As per the curve of PDOP and the number of received satellites shown in Fig. 8, the initialization completion time of the controller was 14.48s, and the satellite receiver has been positioned normally before 14.48s.

The range, trajectory height and yaw curve of the missile were obtained by reading the recorder data, and it can be seen from Fig. 11 that the recorder starts data recording at 14.48s, indicating that it works normally after receiving and positioning. It can also be seen from Fig. 9 and Fig. 10 that the range and yaw of ZD2 conform to the coordinates of the target point, the impact point deviation is small, and the guidance effect is good.

The actuator control data and feedback data were read to verify whether the actuator works normally. Besides, it can be clearly seen from Fig. 12 that the rudder counter signal obtained after the compensation has better tracking performance compared with the uncompensated one, and the rudder control is normal. Besides, it is no longer necessary to verify the rudder control working condition in the small-range test.

2) TEST DATA ANALYSIS OF SMALL RANGE MISSILE

With the firing angle of 73.43° and the firing direction of 1723mil for ZD5, the actual range was 2156m and the range of target point was 2149.9m. Besides, the longitudinal deviation of the final impact point was 6.1m, and the transverse deviation was −7.5944m. When being launched, the missile flew stably and landed normally, and the data of recorder was normal as well. PDOP and star number were shown in Fig. 13.

As per the curve of PDOP and the number of received satellites shown in Fig. 13, the positioning time of satellite receiver was 6.802s.

Recorder data was read, and it can be seen from Fig. 16 that the recorder starts data recording at 6.802s, and works normally when the satellite is received and positioned. It can also be seen from Fig. 14 and Fig. 15 that the range and yaw of ZD2 were in line with the coordinates of target points, the

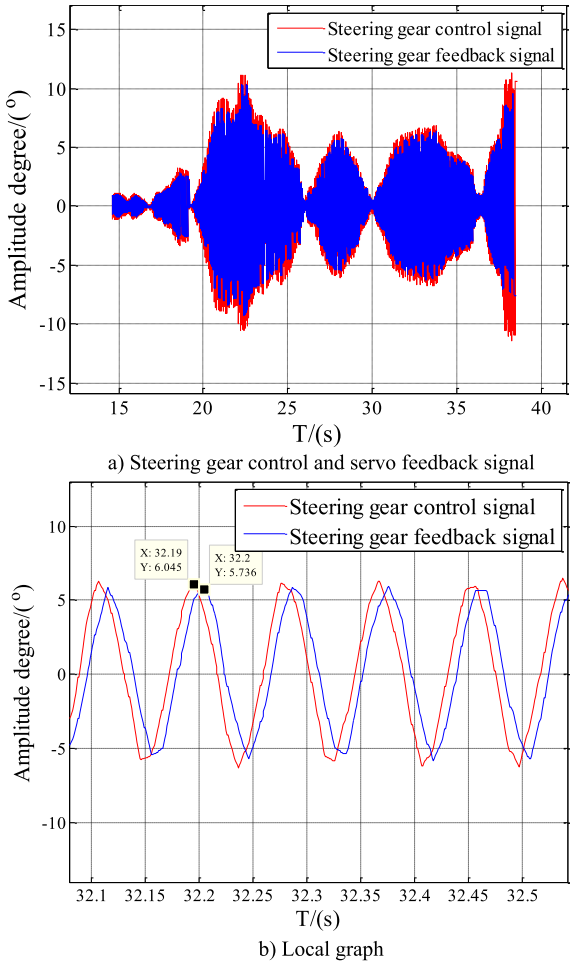

FIGURE 12. Rudder reversal and uncompensated rudder control signals and their Local graph.

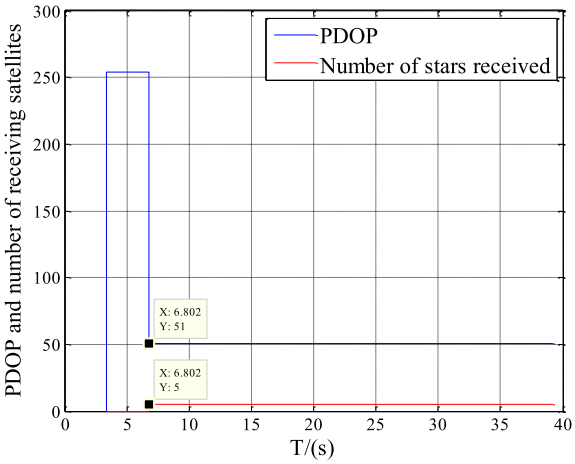

FIGURE 13. PDOP and the number of receiving satellites in small range.

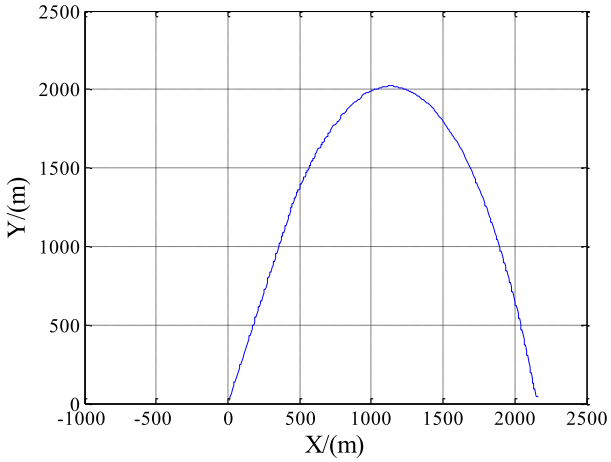

FIGURE 14. Range-Trajectory height curve.

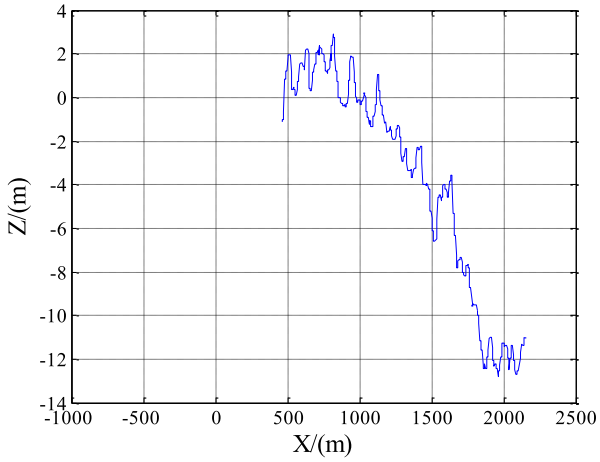

FIGURE 15. Range-Lateral deflection curve.

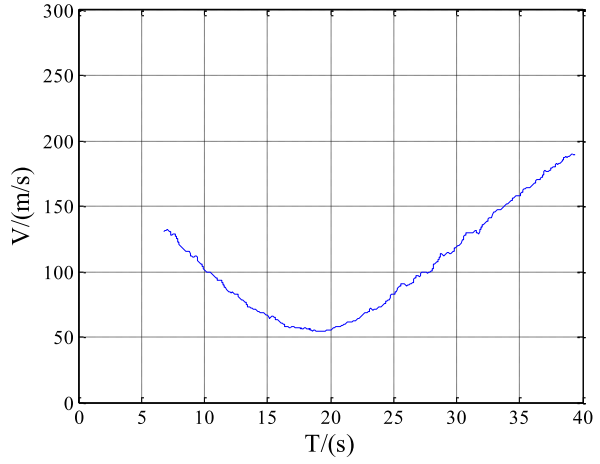

FIGURE 16. Time-Velocity curve.

impact point deviation was small, and the guidance effect was good. As per Fig. 15, the final impact point deviation was about −10.5m, however, the actual value was −7.5944m due to the hardware error. According to the landing point data of multiple missile flight tests, the firing CEP was about 10m. Besides, the accuracy met the requirements, which indicated that the designed guidance law was reasonable and effective.

The improved perturbation guidance was adopted in the ascending section of longitudinal plane, while the adaptive proportional navigation law was adopted in the descending

arc section of longitudinal plane. Besides, the adaptive proportional differential guidance law was used in the transverse plane. As per the results of simulation and flight tests, the integrated guidance can be used to achieve trajectory correction within the whole range and mitigate the impact point dispersion. In the simulation test, CEP not under control decreased from 126.317m 10.1284m when control was applied, which showed that the guidance algorithm was available to effectively resist the interference and improve the accuracy. In the test, the impact point deviation of large, medium and small range was slightly higher than 10m. In most case, it was below 10m, or even less than 1m. The designed guidance algorithm is available to meet the flight requirements of the actual missile, and effectively mitigate the impact point deviation in the application under actual environment. Besides, the CEP was reduced to 10.86m.

VI. CONCLUSION

Thanks to the establishment of 6-DOF trajectory model and control model, an improved perturbation impact point deviation prediction guidance method was constructed in the trajectory rising arc phase. While in the descending arc, the adaptive proportional navigation was constructed in the longitudinal plane, and the adaptive proportional differential guidance law was constructed in the transverse plane. Besides, the simulation results obtained from Monte Carlo simulation of shooting showed that the integrated guidance law was available to significantly mitigate the impact point deviation, and improve the accuracy under the influence of comprehensive deviation. The CEP not under control decreased from 126.317m to 10.1284m when control was applied. On the other hand, the feasibility of the guidance method in engineering application was verified by the flight test. The results showed that the impact point deviation of large, medium and small range was about 10m, even less than 2m. Besides, CEP was reduced to 10.86m, therefore, the guidance method was feasible.

REFERENCES

[1] Y. Zhang *et al.*, "A review on development of foreign guided mortar projectile," *J. Projectiles, Rockets, Missiles Guid.*, vol. 32, no. 6, pp. 24–31, Jun. 2020, doi: 61.1234.TJ.20200618.1353.012.

[2] M. Zhang, D. Liu, D. Wang, and Y. Pang, "A summary for trajectory correction projectiles," *Acta Armamentarii*, vol. 31, no. 12, pp. 127–130, Dec. 2010.

[3] W. Huang and M. Gao, "Development and key technologies of precision guidance module," *Aerodynamic Missile J.*, vol. 12, no. 8, pp. 56–58, Aug. 2016, doi: 10.16338/j.issn.1009-1319.2016.08.12.

[4] S. X. Zhu and D. M. Shi, "Development status and key technology of guided mortar shell," *Aerodynamic Missile J.*, vol. 12, no. 4, pp. 67–70, Apr. 2016, doi: 10.16338/j.issn.1009-1319.2016.04.17.

[5] Z. F. Ke and W. D. Song, "Development status and key technologies of two-dimensional ballistic correction components," *Aerodynamic Missile J.*, vol. 14, no. 5, pp. 81–85, May 2018, doi: 10.16338/j.issn.1009-1319.20170330.

[6] T.-H. Kim, C.-H. Lee, M.-J. Tahk, and I.-S. Jeon, "Biased PNG law for impact-time control," *Trans. Jpn. Soc. Aeronaut. Space Sci.*, vol. 56, no. 4, pp. 205–214, Jul. 2013.

[7] Z. W. Mu *et al.*, "New biased proportional guidance law application in air to ground combat," *J. Command Control*, vol. 5, no. 4, pp. 339–343, Dec. 2019, doi: 10.3969/j.issn.2096-0204.2019.04.0339.

[8] J. Gao, Y. H. Jin, and X. F. Yang, "Terminal guidance control based on biased proportional navigation," *J. Chin. Inertial Technol.*, vol. 25, no. 6, pp. 815–820, Dec. 2017, doi: 10.13695/j.cnki.12-1222/o3.2017.06.021.

[9] G. S. Wang *et al.*, "Biased proportional navigation applicable for infrared guidance munitions," *Syst. Eng. Electron.*, vol. 38, no. 10, pp. 2346–2352, Oct. 2016.

[10] J. Huang, Y. A. Zhang, and Y. X. Liu, "A biased proportional guidance algorithm for moving target with impact angle and field-of-view constraints," *J. Astronaut.*, vol. 37, no. 2, pp. 195–202, Feb. 2016, doi: 10.3873/j.issn.1000-1328.2016.02.009.

[11] M. Gao *et al.*, "Improvement of longitudinal trajectory-correction method based on perturbation theory," *J. Ballistics*, vol. 28, no. 2, pp. 29–34, Jun. 2016.

[12] Z. K. Tian *et al.*, "Impact point prediction algorithm based on perturbation theory," *Mod. Defence Technol.*, vol. 42, no. 3, pp. 86–90, Jun. 2014, doi: 10.3969/j.issn.1009-086x.2014.03.016.

[13] C. W. Li, M. Gao, and W. D. Song, "Real-time impact point prediction of rocket projectile based on perturbation theory," *Acta Armamentarii*, vol. 35, no. 8, pp. 1164–1171, Aug. 2014, doi: 10.3969/j.issn.1000-1093.2014.08.005.

[14] C. E. Pu, L. M. Wang, and J. Fu, "A guidance method for two dimensional trajectory correction projectile based on impact point prediction pf EKF," *J. Ordnance Equip. Eng.*, vol. 39, no. 6, pp. 52–57, Jun. 2018, doi: 10.11809/bqzbgcxb2018.06.011.

[15] F. Kumru, E. Altuntas, T. Akca, "Ballistic coefficient learning based impact point prediction of ballistic targets," *IEEE Trans. Aerosp. Electron. Syst.*, vol. 23, no. 6, pp. 181–186, May 2018.

[16] M. Khalil, X. Rui, Q. Zha, H. Yu, and H. Hendy, "Projectile impact point prediction based on self-propelled artillery dynamics and Doppler radar measurements," *Adv. Mech. Eng.*, vol. 5, Jan. 2015, Art. no. 153913.

[17] F. Kumru, T. Akca, and R. S. Acar, "Performance evaluation of nonlinear filters on impact point prediction of ballistic targets," in *Proc. 20th Int. Conf. Inf. Fusion (Fusion)*, Xi'an, China, Jul. 2017, pp. 1–7.

[18] T. H. Kim, B. G. Park, and M. J. Tahk, "Bias-shaping method for biased proportional navigation with terminal-angle constraint," *J. Guid., Control, Dyn.*, vol. 36, no. 6, pp. 1810–1815, Dec. 2013, doi: 10.2514/1.59252.

[19] Y. D. Wang, C. D. Xu, and X. E. Zheng, "Initial value proportional navigation with impact angle constraint and overload constraint," *J. Projectiles, Rockets, Missiles Guid.*, vol. 39, no. 4, pp. 29–36, Aug. 2019, doi: 10.15892/j.cnki.djzdxb.2019.04.008.

[20] J. X. Wang, X. M. Yang, and W. Wang, "Optimization design of proportional navigation guidance law with gravity over compensation based on guided projectile," *J. Ordnance Equip. Eng.*, vol. 38, no. 7, pp. 67–88, Jul. 2017, doi: 10.11809/scbgxb2017.07.014.

[21] B. S. Kim, J. G. Lee, and H. S. Han, "Biased PNG law for impact with angular constraint," *IEEE Trans. Aerosp. Electron. Syst.*, vol. 34, no. 1, pp. 277–288, Jan. 1998.

[22] S. K. Shi, J. F. Zhao, and H. You, "Design of bias proportional navigation guidance law for motion target with impact angle constraint," in *Proc. IEEE CSAA Guid., Navigat. Control Conf.*, Aug. 2018, pp. 1–5.

[23] S. Lee, N. Cho, and Y. Kim, "Correction: Impact-time-control guidance strategy with a composite structure considering the seeker's field-of-view constraint," *J. Guid., Control, Dyn.*, vol. 43, no. 10, p. 1983, Oct. 2020.

[24] H.-G. Kim, J.-Y. Lee, H. J. Kim, H.-H. Kwon, and J.-S. Park, "Look-angle-shaping guidance law for impact angle and time control with field-of-view constraint," *IEEE Trans. Aerosp. Electron. Syst.*, vol. 56, no. 2, pp. 1602–1612, Apr. 2020, doi: 10.1109/TAES.2019.2924175.

[25] K. B. Li *et al.*, "Guidance strategy with impact angle constraint based on pure proportional navigation," *Acta Aeronautica et Astronautica Sinica*, vol. 41, no. 8, pp. 29–40, Jun, 2020, doi: 10.7527/S1000-6893.2020.24277.

[26] S. Ma *et al.*, "BPNG law with arbitrary initial lead angle and terminal impact angle constraint and time-to-go estimation," *Acta Armamfntarii*, vol. 40, no. 1, pp. 68–78, Jan. 2019.

[27] C.-K. Ryoo, H. Cho, and M.-J. Tahk, "Optimal guidance laws with terminal impact angle constraint," *J. Guid., Control, Dyn.*, vol. 28, no. 4, pp. 724–732, Jul. 2005.

[28] A. Ratnoo and D. Ghose, "State-dependent Riccati-equation-based guidance law for impact-angle-constrained trajectories," *J. Guid., Control, Dyn.*, vol. 32, no. 1, pp. 320–325, Jan. 2009, doi: 10.2514/1.37876.

[29] A. Ratnoo and D. Ghose, "Impact angle constrained interception of stationary targets," *J. Guid., Control, Dyn.*, vol. 31, no. 6, pp. 1816–1821, Nov. 2008, doi: 10.2514/1.37864.

[30] V. Devan and D. Deb, "A new nonlinear guidance law formulation for proportional navigation guidance," in *Proc. 12th Int. Workshop Variable Struct. Syst.*, Jun. 2012, pp. 190–195, doi: 10.1109/VSS.2012.6163500.
[31] D. Viswanath, S. Krishnaswamy, and D. Deb, "Homing missile guidance using LOS rate and relative range measurement," in *Proc. Annu. IEEE India Conf. (INDICON)*, Dec. 2015, pp. 1–6, doi: 10.1109/INDICON.2015.7443715.
[32] D. Viswanath and D. Deb, "Disturbance observer based sliding mode control for proportional navigation guidance," *IFAC Proc. Volumes*, vol. 45, no. 1, pp. 163–168, 2012, doi: 10.3182/20120213-3-IN-4034.00031.
[33] X. F. Qian, *Missile Flight Mechanics*. Beijing, China: Beijing Institute of Techinology, 2016, pp. 2–49.
[34] Z. P. Han, *Exterior Ballistics*. Beijing, China: Beijing Institute of Techinology, 2008, pp. 23–150.
[35] M. Gao, Y. Zhang, and S. Yang, "Firing control optimization of impulse thrusters for trajectory correction projectiles," *Int. J. Aerosp. Eng.*, vol. 2015, Apr. 2015, Art. no. 781472, doi: 10.1155/2015/781472.
[36] Y. W. Zhang, "Research theory and technology of flight control of the trajectory correction mortar projectile," Ph.D. dissertation, Dept. Missile. Eng., Ordnance Eng. College, Shijiazhuang, China, 2016.
[37] Z. C. Lu, M. Gao, and C. N. Jia, "Braking control model and simulation for precision guided kit," *J. Projectiles, Rockets, Missiles Guid.*, vol. 36, no. 2, pp. 97–101, Apr. 2016, doi: 10.15892/j.cnki.djzdxb.2016.02.024.
[38] C. W. Li, "Research on impact point prediction and control technology of trajectory correction rocket," Ph.D. dissertation, Dept. Missile. Eng., Ordnance Eng. College, Shijiazhuang, China, 2014.
[39] H. Z. Wu, M. Gao, and Y. Wang, "Dynamic threshold correction method of trajectory deviation based on perturbation theory," *J. Ballistics*, vol. 32, no. 2, pp. 22–28, Jun. 2020, doi: 10.12115/j.issn.1004-499X(2020)02-004.
[40] Y. Zhang, M. Gao, S. Yang, and D. Fang, "Optimization of trajectory correction scheme for guided mortar projectiles," *Int. J. Aerosp. Eng.*, vol. 2015, Dec. 2015, Art. no. 618458, doi: 10.1155/2015/618458.
[41] G. M. Siouris, *Missile Guidance and Control Systems*. New York, NY, USA: Springer, 2004, pp. 113–188.
[42] Y. W. Zhang, M. Gao, and S. C. Yang, "A practical adaptive proportional-derivative guidance law," *Eng. Lett.*, vol. 24, no. 3, pp. 347–352, Aug. 2016.
[43] Y. W. Zhang, M. Gao, and S. C. Yang, "An adaptive proportional navigation guidance law for guided mortar projectiles," *J. Defense Model. Simul., Appl., Methodol., Technol.*, vol. 13, pp. 1–9, Jun. 2016, doi: 10.1177/1548512916647810.

XITONG SUN was born in Binzhou, Shandong, China, in 1991. He received the bachelor's degree in ammunition engineering and the master's degree in weapon science and technology from the College of Mechanical Engineering, in 2014 and 2016, respectively. He is currently pursuing the Ph.D. degree in weapons science and technology with Army Engineering University.

His research interests include information sensing and control technology, ammunition guidance and control theory, and wireless transmission of near-field electromagnetic signals. He has published seven articles and won the title of excellent student.

MIN GAO was born in Yuncheng, Shanxi, China, in 1963. He received the bachelor's degree in ordnance engineering from the College of Mechanical Engineering, in 1983, and the master's and Ph.D. degrees later.

Since 1983, he has been an Assistant Teacher with the College of Mechanical Engineering. He is currently a Professor and Ph.D. Supervisor, and had guided more than 100 master's and Ph.D. students. He has published more than 100 articles at home and abroad, and is an expert in this field. His research interests include infrared image terminal guidance technology, missile and rocket information theory and technology, guidance, and control theory and technology.

XIAODONG ZHOU was born in Jiujiang, Jiangxi, China, in 1976. He received the Ph.D. degree in mechanical and electrical engineering from the Nanjing University of Science and Technology, in 2005.

Since 2005, he has been teaching at Army Engineering University, where he is currently an Associate Professor. He has published more than ten academic articles. His research interests include new ammunition concept technology, near-field electromagnetic induction technology, phased array radar detection, and millimeter wave detection.

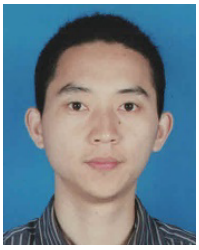

JING LV was born in Zhijiang, Hubei, China, in 1980. He received the bachelor's degree in ammunition engineering from the College of Mechanical Engineering, in 2003, and the master's degree in mechanical engineering, in 2005. He is currently pursuing the Ph.D. degree with the School of Mechatronical Engineering, Beijing Institute of Technology.

He has been an Assistant Teacher with the College of Mechanical Engineering, since 2005, where he is currently a Lecturer. His research interests include laser terminal guidance technology, ammunition guidance, and control theory, and has published seven articles.

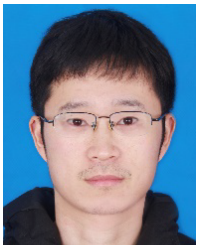

FENG TIAN was born in Nanjing, Jiangsu, China, in 1985. He received the master's degree in control theory and control engineering from Northwestern Polytechnic University, in 2010. Since 2017, he has been a Senior Engineer in System Engineering with the Beijing Aerospace Automatic Control Institute. He is the author of eight articles and holds ten patents. His main research interest includes control systems engineering.

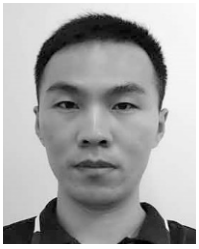

ZHIMING QIAO was born in Handan, Hebei, China, in 1991. He received the B.S. degree from the University of Science and Technology Beijing, China, in 2014, and the M.S. degree from the Shijiazhuang Mechanical Engineering College, Shijiazhuang, China, in 2016.

Since 2016, he has been a Teaching Assistant with the Shijiazhuang Mechanical Engineering College. He has written eight articles, and holds one invention. His research interests include electromagnetic launch, high voltage technology, and modern control system design.